Physics Letters A 373 (2009) 3659–3662

Contents lists available at ScienceDirect

Physics Letters A

www.elsevier.com/locate/pla

Radiographic method for measuring the continuum hard X-ray output spectrum of a Plasma Focus device

V. Raspa *, C. Moreno

Departamento de Física, FCEyN-UBA, PLADEMA-CNEA and INFIP-CONICET, Pab. 1, Ciudad Universitaria, (1428) Buenos Aires, Argentina

ARTICLE INFO

Article history:
Received 7 July 2009
Accepted 18 July 2009
Available online 22 July 2009
Communicated by F. Porcelli

PACS:
52.59.Px
52.58.Lq
87.59.-e
52.38.Ph

Keywords:
Plasma hard X-ray sources
Plasma Focus
Hard X-ray spectrum
Radiographic method

ABSTRACT

A radiographic method is proposed and then applied to infer the continuum part of the hard X-ray spectrum of a 4.7 kJ Plasma Focus from differential absorption measurements on metals. Copper, nickel, titanium and silver samples with thicknesses spanning between 0.1 and 10 mm were employed as filters. The X-ray radiation was detected using a standard radiographic screen-film system. The results show the presence of a dominant peak around 75 keV with significant spectral components in the range of 40 to 200 keV. The method is easy to follow, inexpensive, and allows for calibrated, single shot, spectral measurements.

1. Introduction

Plasma Focus devices are intense sources of polychromatic hard X-ray pulses with extremely short wavelength components (~ 10 pm) and a very short pulse duration (~ 50 ns FWHM) [1], that make them specially suited for a number of important applications [2]. Nanosecond resolution radiographies of metallic pieces hidden behind metallic walls that involved 100 keV photons, were reported among them [3]. The development and enrichment of such imaging applications, as well as the understanding of many Plasma Focus pinch phenomena, benefit with the knowledge of the hard X-ray source spectral characteristics.

Efforts were undertaken in the past to measure the spectrum emitted by Plasma Focus devices in the region of 100 keV using either K-5 nuclear emulsions [4] or differential absorption spectrometry based on thermoluminescence dosimeters (TLD) [5]. In both cases the photon spectrum was indirectly obtained, since it was calculated after an electron spectrum compatible with the recorded data, was determined. Ross filters coupled to photodetectors were also used, but so far they allowed to analyze photon energies up to 67.4 keV [4,6,7], which is the K-shell absorption edge of tantalum.

A TLD-based multichannel absorption spectrometer was proposed in 2004 by Tartari et al. [8] to analyze the X-ray output of a Plasma Focus using each TLD both as detector and absorber. Photon energies between 5 and 45 keV were reported, and about 40 shots were required to improve the signal-to-noise ratio. More recently, an effective, single shot, Plasma Focus hard X-ray spectrum was determined from attenuation data on metallic samples [3] following a method that allows for comparisons between measurements made on different devices, provided that the same type of hard X-ray detector is used.

In the current communication, a method based on differential absorption on metallic plates and the standard densitometry of their radiographs, is proposed. The method incorporates a direct way to relate optical densities measured on the film, with the corresponding film exposures, thus avoiding the necessity of using the same type of radiographic detectors to make comparisons. The method is afterwards applied to determine the continuum part of the hard X-ray spectrum of a 4.7 kJ Mather-type tabletop Plasma Focus device.

2. Method

2.1. Hard X-ray detector

High sensitivity orthochromatic AGFA X-ray film along with terbium-doped gadolinium oxysulphide (Gd_2O_2S:Tb) intensifying

* Corresponding author. Tel.: +54 11 4576 3371 ext. 122; fax: +54 11 4576 3357.
E-mail address: raspa@df.uba.ar (V. Raspa).

0375-9601/$ – see front matter
doi:10.1016/j.physleta.2009.07.046

screens is proposed as hard X-ray detector, since it is widely used for radiographic applications. In this screen-film system, the X-ray film is impressed by visible photons emitted by the intensifying screens which basically act as transducers from hard X-rays to visible light. The X-ray film itself is placed inside a 13×18 cm^2 light-tight to visible radiation cassette whose internal walls are coated by individual soft thin pads that contain the Gd_2O_2S:Tb transducer. Such pads are commonly referred to as intensifier screens. The visible light emitted by the intensifier screens has a band spectrum dominated by photons of ~ 540 nm (green), being the next two relevant bands located at 480 and 580 nm, respectively, each one with a relative intensity of 0.34 with respect to the maximum [9]. The spectral sensitivity of the orthochromatic X-ray film spans from 300 to 580 nm, and therefore it matches the spectral output of the intensifier screen. The film itself is insensitive to hard X-rays and to wavelengths longer than 650 nm (red).

2.2. Formulation of the method

The amount of visible photons per unit area impressing the film due to the transmission of the hard X-ray polychromatic beam through an arbitrary sample of thickness d is defined as

$$I(d) \equiv \int_0^\infty A\eta(E)S(E)e^{-k(E)d}\,dE \tag{1}$$

where A is the total amount of hard X-rays photons reaching the screens per unit area, $\eta(E)$ is the screen conversion efficiency [3,10] and $S(E)$ is the continuum part of the unknown hard X-ray spectrum. Expression (1) considers that the intensity of each spectral component exponentially decays as it penetrates matter. In that case, a linear attenuation coefficient, $k(E)$, depending on the sample material, characterizes the radiation decay. Values of $k(E)$ from 1 keV to 20 MeV for elements $Z = 1$ to 92 are tabulated in Ref. [11]. To get rid off the unknown quantity A, the following transmission coefficient $T(d)$ can be considered

$$T(d) \equiv \frac{I(d)}{I(0)} = \frac{\int_0^\infty \eta(E)S(E)e^{-k(E)d}\,dE}{\int_0^\infty \eta(E)S(E)\,dE}. \tag{2}$$

For a set of metallic samples made of different materials and thicknesses, Eq. (2) can be expressed as

$$T_{ij} \equiv \frac{\int_0^\infty \eta(E)S(E)e^{-k_i(E)d_{ij}}\,dE}{\int_0^\infty \eta(E)S(E)\,dE}, \tag{3}$$

where T_{ij} is the transmission coefficient for the sample j made of material i; $k_i(E)$ and d_{ij} are, respectively, the linear attenuation coefficient and thickness of the ij sample.

The standard weighted least-squares method can be used to infer a point-defined function $S(E)$ by minimizing the functional χ^2 defined as

$$\chi^2 \equiv \sum_{i,j} w_{ij}\left(T_{ij}^{\text{meas}} - T_{ij}\right)^2, \tag{4}$$

where the right term of Eq. (4) evaluates the accordance between the transmission values prescribed by expression (3) and the corresponding measured values T_{ij}^{meas}, being $w_{ij} = \sigma_{ij}^{-2}$ a weighting factor that accounts for the experimental uncertainty, σ_{ij}, of T_{ij}^{meas}.

2.3. Implementation of the method

Since the screen-film detection system gives no direct information on T_{ij}^{meas} but rather on optical densities, we propose to place, between each intensifier screen and the film, a set of calibrated gray filters for the visible light emitted by the screens; in such a way that after exposing the detection system to the hard X-rays, a calibration between known absolute transmissions and measured optical densities can be performed. The proposed transmission set is from AGFA, model Structurix Denstep 30, which is a certified density step wedge film covering optical densities from 0.152 to 4.230 in 15 steps. For the application reported in Section 3, the first eight steps of such set was used, providing transmissions values, T, in the range of 0.074 to 0.700.

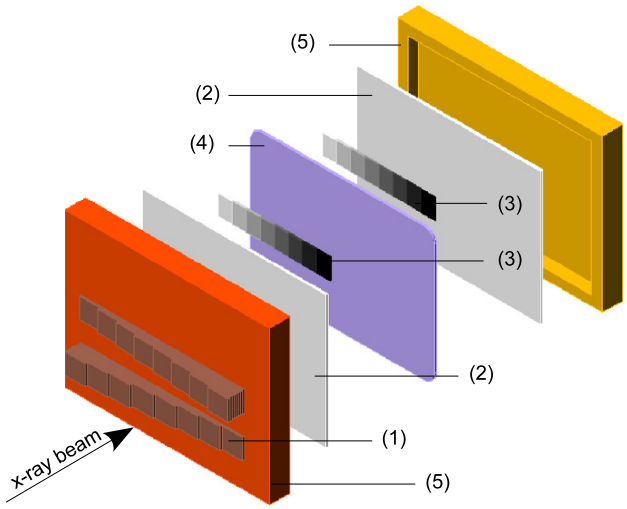

Fig. 1. Exploded sketch of the detection system. For the figure simplicity, only two sets of metallic plates are illustrated. Refs.: (1) metallic plates, (2) intensifier screen, (3) calibrated transmission set, (4) X-ray film, (5) light-tight plastic cassette body.

Fig. 1 presents an exploded sketch of the proposed detection system where the layout of the intensifier screens, the transmission sets and the film, are also shown. For the figure simplicity, only two sets of metallic plates facing the X-ray beam are illustrated.

The following normalized optical density (NOD) can be used to take eventual film inhomogeneities into account

$$\text{NOD}_{ij} \equiv \frac{\text{OD}_{ij}}{\text{OD}_{ij}^B}, \tag{5}$$

where OD_{ij} is the optical density measured for sample ij and OD_{ij}^B is the optical density of the nearby background.

3. Application example

The above presented method was applied to measure the continuum part of the hard X-ray emission of a small-chamber Mather-type plasma focus device. The facility stores 4.7 kJ when charged at 30 kV. The device was operated using a total pressure of 3.5 mbar of a deuterium–argon mixture (2.5% of argon by volume) as working gas. The output window for the hard X-ray radiation is a 0.75 mm thick stainless steel flat disk, which is also the front end of the discharge chamber. Additional details of the device can be found elsewhere [3,12,13].

The used set of plates is detailed in Table 1, and a single shot radiograph of them, when placed at 70 cm from the chamber front wall, is shown in Fig. 2. Samples were grouped by material and sorted by decreasing thickness either from right to left (for copper, nickel and titanium) or from top to bottom (silver). Different tonalities can be appreciated according to the plate material and thickness. Two lead samples were used to determine the fog level reference.

Table 1
Materials and thicknesses of the used samples. Thicknesses uncertainty is ±0.01 mm.

Material	Thicknesses [mm]
silver	from 0.10 to 0.80, in eight 0.10 steps
titanium	from 0.89 to 9.79, in eleven 0.89 steps
copper	from 0.20 to 3.00, in fifteen 0.20 steps
nickel	from 0.15 to 3.00, in twenty 0.15 steps
lead	14.00 and 18.80

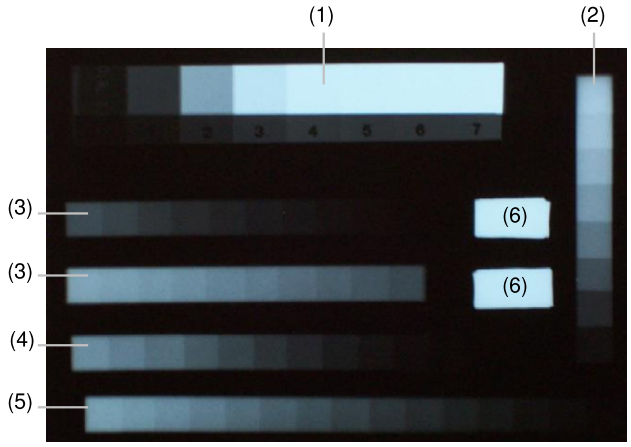

Fig. 2. Single-shot radiographic image of the plates set used to determine the radiation spectrum. Refs.: (1) calibration image, (2) silver, (3) nickel, (4) titanium, (5) copper and (6) fog level reference.

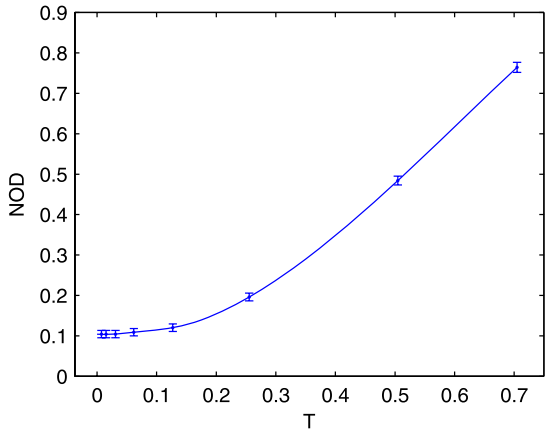

Fig. 3. Calibration data obtained from the densitometric analysis of the image on the top of Fig. 2.

The calibration data shown in Fig. 3 were determined from the densitometric analysis of the calibration image on top of Fig. 2 and the calibrated transmission values of the Denstep 30. Each T_{ij}^{meas} value was obtained interpolating the calibration data for the corresponding normalized optical density.

An optical transmission densitometer was used to measure the optical density of each sample image and the corresponding background. Fig. 4 illustrates the normalized optical density for the considered samples as a function of the sample thickness d_{ij}. All the processed radiographs verify that the film exposure was above the film fog level (which correspond to OD = 0.2) and well below the saturation level (OD = 3.5) [14].

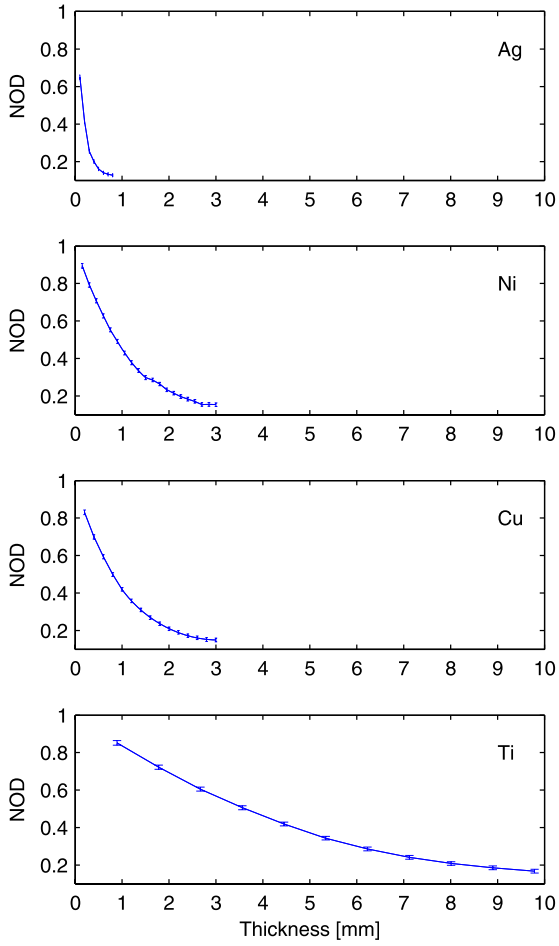

Fig. 4. Normalized film optical density for the considered metallic samples as a function of the sample thickness.

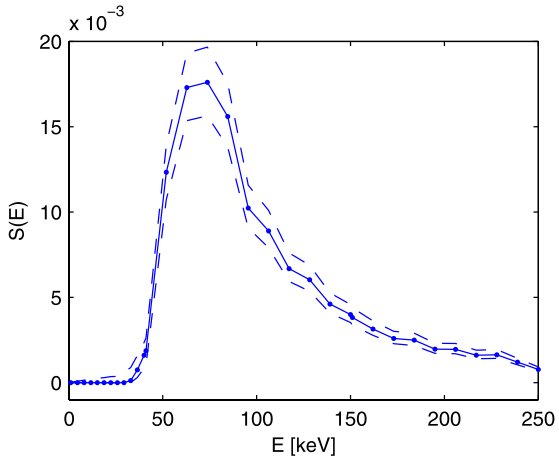

Fig. 5. Obtained X-ray continuum spectrum. Dashed curves indicate error bands.

3.1. Results

The obtained spectrum together with the corresponding error bands are presented in Fig. 5 in full and dashed lines respectively. Linear filtering was used to get smooth results. As it can be observed, the spectral amplitude is practically null below 40 keV.

It then rapidly grows up at higher energies, reaching a single maximum located close to 75 keV, becoming negligible beyond 200 keV. The error bands were estimated by means of the Monte Carlo Method [15]. The input data (that is: the measured values of T_{ij}^{meas} as well as the corresponding thicknesses d_{ij}) were randomly perturbed within their own error bands for each material. A perturbed spectrum $S_n(E)$ was afterwards evaluated from such simulated data. A number of $n = 10\,000$ realizations of these calculations gave a set of spectra $S_n(E)$, $1 \leqslant n \leqslant 10\,000$, which, once plotted together with $S(E)$, gave a broad region, delimited by the dashed curves reported as error bands in Fig. 5.

As a cross-check of the above described numerical method, the zeroth-order regularization method [15] was also followed to determine a function $S(E)$. Considering regularization parameters between 0 and 10^{-3}, the obtained results are coincident with the solution showed in Fig. 5. Again, numerical filtering was used to get smooth spectral functions.

4. Conclusions

A radiographic method was presented and applied to measure the continuum hard X-ray spectrum emitted by a 4.7 kJ Plasma Focus device optimized for hard X-ray imaging applications. The resulted spectrum presents a maximum around 75 keV, and a spectral bandwidth covering the 40–200 keV region. The obtained lower energy limit is consistent with the fact that spectral components below 40 keV are strongly attenuated by the chamber front wall. The examined radiation proved to be well suited for good contrast radiography of different materials. Such fact, compatible with a broadband probing radiation, is consistent with the obtained spectrum. Filter materials and thicknesses and/or calibrated transmission sets can be adapted to explore the hard X-ray output of other devices having, for instance, different spectral characteristics and/or emission intensities.

Since only the use of standard materials and numerical procedures are required, the presented method is inexpensive and easy to be applied. The use of Ross filters (not always available for energies around 100 keV or above) and TLD calibration and postprocessing are circumvented. Moreover, the sensitivity of currently available standard cassettes and X-ray films is high enough to make the proposed method suitable for widespread use even in single shot spectral measurements.

Acknowledgements

This work was supported by UBA (Projects X810 and X152), and CONICET. V.R. and C.M. are Doctoral fellow and member of CONICET, respectively.

References

[1] A. Bernard, H. Bruzzone, P. Choi, H. Chuaqui, V. Gribkov, J. Herrera, K. Hirano, A. Krejëi, S. Lee, C. Luo, F. Mezzetti, M. Sadowski, H. Schmidt, K. Ware, C.S. Wong, V. Zoita, J. Moscow Phys. Soc. 8 (1998) 93.
[2] V.A. Gribkov, AIP Conf. Proc. 996 (2008) 51.
[3] V. Raspa, C. Moreno, L. Sigaut, A. Clausse, J. Appl. Phys. 102 (2007) 123303.
[4] H. van Paassen, R. Vandre, R. White, Phys. Fluids 13 (1970) 2606.
[5] N. Filippov, et al., IEEE Trans. Plasma Sci. 24 (1996) 1215.
[6] D. Johnson, J. Appl. Phys. 45 (1974) 1147.
[7] M. Shafiq, S. Hussain, A. Waheed, M. Zakaullah, Plasma Sources Sci. Technol. 12 (2003) 199.
[8] A. Tartari, A. Da Re, C. Bonifazzi, M. Marziani, Nucl. Instrum. Methods Phys. Res., Sect. B 213 (2004) 206.
[9] S. Duclos, Electrochem. Soc. Interface 7 (1998) 34.
[10] B. Illerhaus, Y. Onel, J. Goebbels, Proc. SPIE 5535 (2004) 329.
[11] J. Hubbell, S. Seltzer, X-rays attenuation coefficients, NIST, 1996, http://physics.nist.gov/PhysRefData/XrayMassCoef/cover.html.
[12] C. Moreno, M. Vénere, R. Barbuzza, M. Del Fresno, R. Ramos, H. Bruzzone, F.P.J. González, A. Clausse, Braz. J. Phys. 32 (2002) 20.
[13] C. Moreno, H. Bruzzone, J. Martínez, A. Clausse, IEEE Trans. Plasma Sci. 28 (2000) 1735.
[14] CP-G Film datasheet, Agfa-Gevaert N.V., Belgium (2004).
[15] W.H. Press, B.P. Flannery, S.A. Teukolsky, W.T. Vetterling, Numerical Recipes in C: The Art of Scientific Computing, second ed., Cambridge Univ. Press, New York, 1988.